unpublished report of April, 1958, which the authors were privileged to review, served as a basis for this study.

NOTATION

a,k = empirical constants
D = impeller diameter, in.
N = shaft speed, rev./min.
t = agitation time, min.
T = tank diameter, in.
ω = peripheral speed, ft./min.
μ_t = arithmetic mean particle diameter at time t, μ
μ_∞ = ultimate particle diameter, μ
$\Delta\mu$ = deviation from ultimate particle diameter, μ

LITERATURE CITED

1. Bates, R. L., *Ind. Eng. Chem.*, **51**, 1256-8 (1959).
2. Brothman, A., *Chem. and Met.*, **46**, No. 5, p. 263-5 (1939).
3. Calderbank, P. H., *Brit. Chem. Eng.*, **1**, 206-9, (August, 1956).
4. ———, *Trans. Inst. Chem. Engrs. (London)*, **36**, 443-63 (1958).
5. Clayton, W., "The Theory of Emulsions and Their Technical Treatment," 5 ed., The Blakiston Co., New York (1954).
6. Herschel, W. H., "Technologic Papers of the Bureau of Standards," Vol. 86, pp. 1-37 (1917).
7. Hinze, J. O., *A.I.Ch.E. Journal*, **1**, No. 3, p. 289-95 (1955).
8. Miller, F. D., and J. H. Rushton, *Ind. Eng. Chem.*, **36**, 499-503 (1944).
9. Morton, A. A., and L. M. Redman, *ibid.*, **40**, 1190-3 (1949).
10. Oldshue, J. Y., "Biological Treatment of Sewage And Industrial Wastes," Vol. 1, p. 233, J. McCabe and W. W. Eckenfelder, Reinhold, New York (1955).
11. Rodger, W. A., V. G. Trice, Jr., and J. H. Rushton, *Chem. Eng. Progr.*, **52**, 515-20 (1956).
12. Scoville, W. L., "The Art Of Compounding," The Blakiston Co., New York (1895).
13. Vermeulen, Theodore, G. M. Williams, and G. E. Langlois, *Chem. Eng. Progr.*, **51**, 85F-94F (1955).

Manuscript received May 8, 1961; revision received August 20, 1962; paper accepted August 22, 1962. Paper presented at A.I.Ch.E. Cleveland meeting.

Flow and Diffusion Characteristics of Alumina Catalyst Pellets

J. L. ROBERTSON and J. M. SMITH

Northwestern University, Evanston, Illinois

Steady state constant pressure diffusion measurements were made on a series of alumina pellets using the nitrogen-helium system at 1 atm. and 80°F. The pellets were prepared from the same alumina powder but compressed to different densities. Pore size distribution data indicate that all the pellets had approximately the same micropore sizes and volume, but different macropore volumes. Flow measurements with nitrogen were also carried out for the same pellets over a pressure range, up to 1 atm. The data show that the pellet density, or macropore volume, has a pronounced effect.

On the basis of a simplified model of the pellet, path lengths were evaluated from the flow data. On the assumption that the diffusion path length is the same, a method is presented for predicting diffusion rates. The results so computed are independent of the path tortuosity. The method correctly evaluates the effect of pellet density on diffusion, but measured rates are 40 to 80% of the calculated values.

FLOW AND DIFFUSION CHARACTERISTICS OF ALUMINA CATALYST PELLETS

In the recent literature attention has been given to calculation of effectiveness factors for reactions in porous catalysts *(1, 2, 10, 14)*. The parameters used in these calculations contain the transport coefficients for heat and mass transfer. It is therefore important to know the magnitude of these coefficients in order to calculate the effectiveness of a particular catalyst system. Data for experimentally determined diffusivities have been published by Weisz *(13)*, Hoogschagen *(7)*, and Wicke and Kallenbach *(15)*, among others. Henry, Chennakesavan, and Smith *(5)* have presented data for diffusion of nitrogen, helium, and carbon dioxide through a porous alumina pellet. From the ratio of the diffusion rates observed it was concluded that Knudsen flow controlled the process. However it has since been shown *(12)* that this is not a satisfactory criterion for determining the mechanism of diffusion. Masamune and Smith *(9)* have presented data for diffusion of helium and nitrogen through porous silver catalysts. The results indicated that diffusion was primarily through the relatively large macropores.

This paper presents diffusion and flow data through alumina pellets of widely different pore size distributions with the objective of evaluating the effect of geometry of the porous pellet on its mass transfer characteristics. The flow measurements were made at atmospheric pressure, or below, with nitrogen, while diffusion was studied at atmospheric pressure with the nitrogen-helium system. From a model of the pellet a method is developed for predicting the diffusion rate from flow measurements.

PELLET PROPERTIES

Cylindrical pellets were made by compressing alumina monohydrate (Boehmite) powder into pellets of different densities. The average size (with respect to weight) of the particles of the powder used for pellets 1 to 6 was about 85 μ. For pellet 7 the average size is estimated to be 700 μ. The pellets were all 2 cm. in diameter and about 1 cm. in length. Pellets made with the same amount of powder exhibited about 1 to 2% deviation in density.

Figure 1 gives the cumulative pore volume, as measured by nitrogen desorption (for pores smaller than 500 Å.) and mercury porosimeter (for pores whose openings are greater than 500 Å.).* Pellets 1 to 6 were made with the same powder by compressing different quantities to the same size pellet. The least-dense pellet, which had a total pore volume of 1.64 cc./g., was compressed at about 2,000 lb./sq. in. This was the minimum compression pressure necessary to make a pellet of sufficient strength for handling. The most dense pellet was compressed at a pressure of about 50,000 lb./sq.

J. L. Robertson is with the Esso Research and Engineering Company, Linden, New Jersey. J. M. Smith is with the University of California, Davis, California.

* Mr. M. F. L. Johnson, Sinclair Research Laboratories, Harvey, Illinois, determined the pore volume data and also calculated the distribution results, shown in Figure 2, from these data.

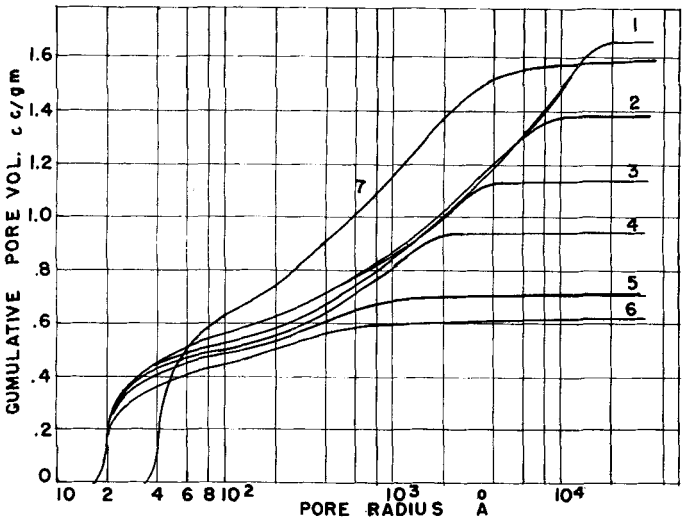

Fig. 1. Cumulative pore volume of catalyst pellets.

in., the upper limit of the Carver press (model B). Pellet 7 is the one for which diffusion data were reported by Henry, Chennekesavan, and Smith (5).

To establish the volume in pores of certain sizes the derivative of the curves shown in Figure 1 was taken. The results are shown in Figure 2 for pellets 1, 6, and 7. Curves for pellets 2 to 5 were between those for 1 and 6. It is evident from this figure that there are two types of pore distributions that make up the internal volume of alumina pelleted catalysts. One of these is due to the micropores within the powder particles and is represented by the peak at 20 Å. for pellets 1 to 6 and at 40 Å. for pellet 7. The other type of distribution represents the macropores between powder particles and shows peaks between 500 and 10,000 Å., depending on the particle size distribution of the powder used and the pellet density. The minimum in the derivative curve was chosen to represent the separation between macropores and micropores. This corresponds to 100 Å. for pellets 1 to 6 and 180 Å. for pellet 7.

Table 1 gives a summary of the physical properties of the pellets. As the pellet density increased, the macropore volume was reduced from 1.08 to 0.18 cc./g. aluminum oxide* in pellets 1 to 6. However the micropore volume and surface area of pellets 1 to 5 remained essentially constant and decreased only slightly for pellet 6. This indicated that increasing pelleting pressure influenced only the macropores and that the powder particles remain essentially intact during the pelleting. A slight crushing of the powder particles would account for the decrease in micropore volume and surface area for pellet 6.

* X-ray analysis by Mr. Johnson indicated that the alumina powder as pelleted was in the form of α-$Al_2O_3 \cdot H_2O$ that is Boehmite. However the macropore volume is referred to a unit mass of aluminum oxide.

EXPERIMENTAL METHOD

The experimental method for the diffusion measurements is similar to that reported by Weisz (*11*) and Henry et al. (5). Figure 3 shows a schematic drawing of the experimental apparatus. All diffusion measurements were made at approximately 1 atm. total pressure and 80°F. Pure, dry helium and nitrogen are fed through calibrated flowmeters and control valves at about 500 cc./min. to opposite faces of the pellet. The flow rates are so regulated that there is no total pressure drop across the pellet, as observed on the manometer. All capillary flowmeters were calibrated to 1% accuracy or better. The effluent from each side of the cell is fed to the sample side of a thermal conductivity cell. Pure nitrogen or helium is simultaneously passed through the reference side of the cells. During a diffusion run shutoff valves 1, 2, 5, and 6 (Figure 3) are closed. The concentration of the effluent gas streams are determined by noting the steady state voltage reading for each cell. Then shutoff valves 3, 4, 7, and 8 are closed and 1, 2, 5, and 6 are opened. Nitrogen is bled into the helium-rich stream and helium into the nitrogen-rich stream through shutoff valves 1 and 2 until the same voltage readings were obtained as during the diffusion run. These results gave the diffusion rates of the individual gases and also the composition of the gas stream on each side of the pellet. This method of operation eliminates the errors due to calibration of the cells and also gives an independent measurement of the diffusion rate of each gas.

Figure 4 shows the diffusion cell in which the pellets were mounted in slightly undersize tygon tubing and clamped in place with a split ring and hose clamp. Leakage between the pellet and the tygon was low enough to be unmeasurable. The flow of gas was directed tangentially near the pellet face to eliminate kinetic energy effects and the buildup of a stagnant layer.

For flow measurements one side of the diffusion cell was connected to a vacuum system. Then the amount of nitrogen necessary to maintain the other side at some constant pressure was noted along with the total pressure drop across the pellet. Flow data were obtained at several values of total pressure drop and average pressure (up to 1 atm.) in the pellet.

MODEL OF PORE STRUCTURE

Diffusion in porous materials is complicated by the fact that the process in very small pores (Knudsen flow) is different from that in larger pores (bulk diffusion). The Knudsen diffusivity is a function of pore size, and the bulk value is a function of pressure. For the pressure and materials used in this study Knudsen flow would predominate in the micropores within the powder particles, and both the bulk and Knudsen process occur in the macropores between particles in the pellet. It would be expected that the lower resistance offered in the macropore region would result in both flow and diffusion rates being controlled by this region. How-

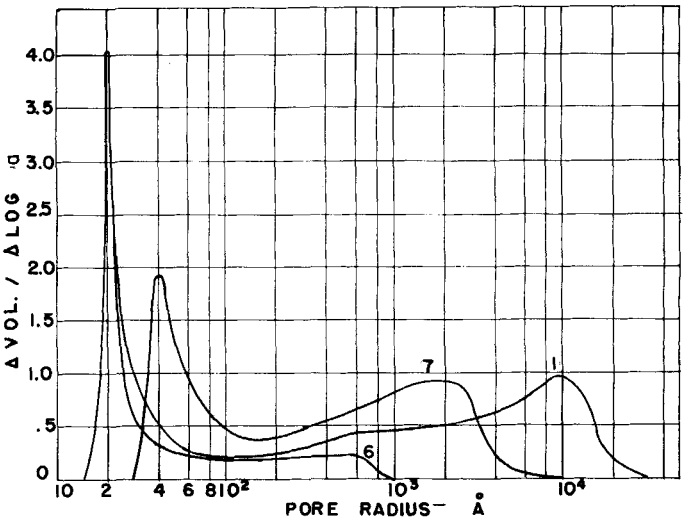

Fig. 2. Pore-size distribution.

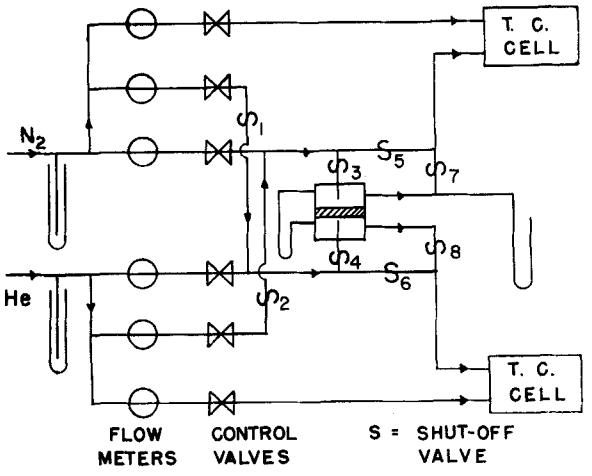

Fig. 3. Diffusion apparatus schematic.

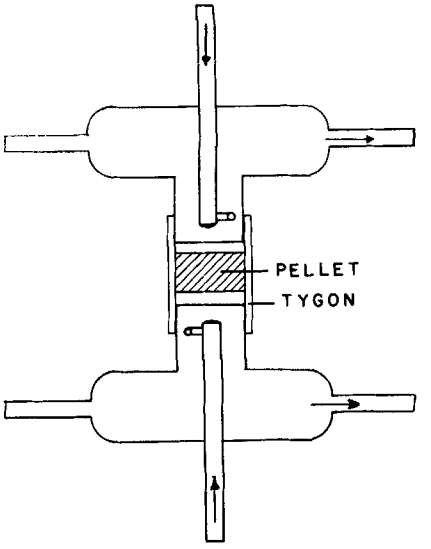

Fig. 4. Diffusion cell detail.

ever it is possible that surface stresses developed during pelleting could result in a thin layer of alumina containing only micropores at each end of the pellet. Equations are presented in the following sections for the situation in which the gases pass through both a macro and micropore region of lengths of L_B and L_K. From the flow data the effective lengths can be evaluated. The relative magnitude of L_B and L_K then serve as a test of the expectation that flow (and presumably diffusion) is predominately in the macropores.

The model for the pellet takes the form shown in Figure 5. The pellet is supposed to contain a layer of microporous material of thickness $L_K/2$ at each face.* This concept does not require that all of the micropore volume is in these surface layers. Indeed nearly all of this volume is within the particles in the pellet. However it is assumed that the micropores in the surface layers have the same pore-size distribution (β_i) as determined for the powder as a whole (shown in Figure 2). It is further assumed in the model that all of the pores of one type are cylindrical, of the same effective length (L_K for micropores and L_B for macropores), and in parallel.

In the equations that follow macropores (designated by j) are those with radii larger than 100 Å. in pellets 1 to 6 and larger than 180 Å. in pellet 7. The micropores (i) are those with smaller radii.

Diffusion through Micropores

In the micropores the pore size is much less than the mean free path, so diffusion follows the Knudsen mechanism. The rate of diffusion for component 1 per gram of aluminum oxide through the n_i pores of radius a_i is

$$Q_{i,1} = n_i \frac{2a_i^3}{3} \frac{8\pi^{1/2}}{M_1 RT} \frac{\Delta P}{L_K} \qquad (1)$$

All of the micropores in the pellet are assumed to have the same length L_M. Only the fraction w occurs in the stressed surfaces of the pellet, so that the length $L_K = wL_M$. The number of pores n_i in Equation (1) is known only in combination with the length L_K from the pore volume distribution data (Figure 2). To utilize these data to determine n_i the micropore distrition function β_i is defined as

$$\beta_i = n_i L_M = n_i L_K/w = \frac{\Delta V_i}{\pi a_i^2} \qquad (2)$$

where ΔV_i is the volume of pores whose radii are from a_i to $a_i + \Delta a_i$. Thus β_i can be determined from the pore size distribution data. Summing Equation (1) for the micropores (a = 0 to a = 100 Å.) one gets the following expression for the total diffusion rate:

$$Q_1 = \frac{\gamma_1 (\Delta p_1) w}{L_K^2} \sum_i \beta_i a_i^3 \qquad (3)$$

where

$$\gamma_1 = \frac{2}{3}\left(\frac{8\pi}{M_1 RT}\right)^{1/2} \qquad (4)$$

Replacing partial pressures with mole fractions, using the ideal gas law and solving Equation (3) for the mole fraction at the boundary between micro and macropores in the model (location 1 on Figure 5), one gets

$$x_{I,1} = x_{o,1} - \frac{Q_1 L_K^2}{w P \gamma_1 \sum_i \beta_i a_i^3} \qquad (5)$$

Diffusion through Macropores

Knudsen as well as bulk diffusion may be significant in the macropores. Scott and Dullien (*12*), Rothfeld (*11*), and Evans, Watson, and Mason (3) have recently developed equivalent equations for predicting the total diffusion rate under such circumstances. The result, in terms of the diffusion flux N_1 of component 1 through a single macropore of length L_B, is

$$N_1 = \frac{P D_{1,2}}{RT(1+\alpha)L_B} \ln \frac{1 + \frac{D_{1,2}}{D_{K,1}} - (1+\alpha)x_{L,1}}{1 + \frac{D_{1,2}}{D_{K,1}} - (1+\alpha)x_{I,1}} \qquad (6)$$

In this expression $D_{K,1}$ refers to the Knudsen diffusivity of component 1 in the macropore of radius a_j. This diffusivity is a function of pore radius; that is

$$D_{K,1} = \frac{2}{3} a_j \bar{v}_1 = \frac{2}{3} a_j \left(\frac{8RT}{\pi M_1}\right)^{1/2} \qquad (7)$$

The ratio of the diffusion rates of the two components is α. For large pore radii Equation (6) reduces to the usual expression for bulk diffusion, and for $\alpha = -1$ the Bosanquet expression (3) for self-diffusion is obtained.

A macropore distribution function β_a can be defined analogous to that for the micropores:

$$\beta_a = n_j L_B = \frac{\Delta V_B}{\pi a_j^2} \qquad (8)$$

In this expression the pore volume distribution ΔV_B vs. a_j is known from the data of Figure 2. With Equation (8) for the number of pores of radius a_j the diffusion rate through all the pores of this radius is

$$Q_{j,1} = \frac{D_{1,2} P \beta_j \pi a_j^2}{RT(1-\alpha)L_B^2}$$

* The diffusion and flow equations to be developed are independent of whether the microporous layer is concentrated at one end of the model, as in Figure 5, or divided into two thicknesses, $L_K/2$ one at each end of the model pellet. This is because the pressure is constant throughout the pellet under the steady state, constant pressure conditions of the experimental method.

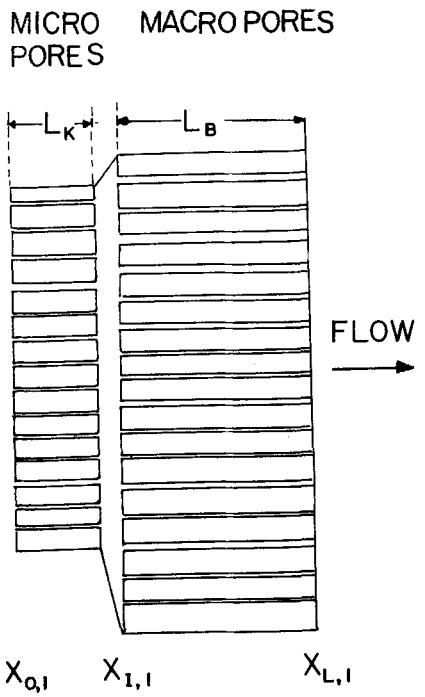

Fig. 5. Model of catalyst pellet.

$$\ln \frac{1 + \frac{D_{1,2}}{D_{K,1}} - (1+\alpha)x_{L,1}}{1 + \frac{D_{1,2}}{D_{K,1}} - (1+\alpha)x_{I,1}} \quad (9)$$

The total diffusion rate per gram of pellet is obtained by summing over the macropore volume:

$$Q_1 = \frac{p\, D_{1,2}\, \pi}{RT(1-\alpha)L_B^2} \sum_j a_j^2 \beta_j \ln \frac{1 + \frac{D_{1,2}}{D_{K,1}} - (1+\alpha)x_{L,1}}{1 + \frac{D_{1,2}}{D_{K,1}} - (1+\alpha)x_{I,1}} \quad (10)$$

This equation may be used to calculate a diffusion rate Q_1 through the pellet, provided the path length factors L_K^2/w and L_B^2 are known. Equation (5) determines the intermediate mole fraction $x_{I,1}$, and the end mole fractions $x_{L,1}$ and $x_{0,1}$ and α are known. The distribution functions β_i and β_j are evaluated from the pore size distribution data. The path-length factors can be calculated from flow data, if it is supposed that the flow and diffusion paths are the same. This is described in the next section.

Flow through Pellets

The equation for flow F through the micropores is identical to that for diffusion except that the partial pressure difference is replaced by the total pressure difference:

$$F = \frac{(\Delta P_K)w}{L_K^2} \gamma_1 \sum_i \beta_i a_i^3 \quad (11)$$

Table 1. Physical Properties of Alumina Pellets

Pellet no.	Pellet diameter, cm.	Pellet thickness, L_p, cm.	Pellet mass, g. Al_2O_3*	Macropore volume, cc./g. Al_2O_3	Micropore volume, cc./g. Al_2O_3	BET (nitrogen) surface area, sq. cm./g. Al_2O_3	Macropore void fraction, ϵ_j
1	2.074	0.924	1.520	1.08	0.56	389	0.528
2	2.078	0.951	1.825	0.81	0.56	419	0.459
3	2.075	0.951	2.120	0.60	0.52	415	0.395
4	2.083	0.914	2.437	0.44	0.50	412	0.345
5	2.083	0.981	2.738	0.265	0.49	381	0.217
6	2.075	0.988	3.200	0.180	0.43	354	0.173
7	2.100	0.899	1.645	0.723	0.74	280	0.382

* g. Al_2O_3 refers to mass of Al_2O_3 as obtained by ignition of actual Boehmite pellets.

For flow through the macropores the slip flow equation is used. This is the Poiseuille equation modified to account for slip at the wall. It is clearly developed by Present (8) and is

$$F = [\eta \sum_j a_j^4 \beta_j + \sigma \sum_j a_j^3 \beta_j] \frac{\Delta P_B}{L_B^2} \quad (12)$$

where

$$\eta = \frac{\pi \bar{P}}{8\mu RT} \quad (13)$$

$$\sigma = \pi \left(\frac{\pi}{8 M_1 RT}\right)^{1/2} \quad (14)$$

The total pressure drop across the model is $\Delta P_K + \Delta P_B$. Solving Equations (11) and (12) for these quantities one gets a relationship between the flow rate and pressure drop as follows:

$$\frac{\Delta P}{F} = \frac{L_B^2}{\eta \sum_j a_j^4 \beta_j + \sigma \sum_j a_j^3 \beta_j} + \frac{L_K^2}{w \gamma_1 \sum_j a_i^3 \beta_i} \quad (15)$$

In accordance with this equation a plot of $\Delta P/F$ vs.

$$[\eta \sum_j a_j^4 \beta_j + \sigma \sum_j a_j^3 \beta_j]^{-1}$$

evaluated at different pressures should give a straight line of slope L_B^2 and an intercept that contains L_K^2/w and the constant, micropore size distribution. Hence flow measurements at several pressures will permit the evaluation of L_B and L_K^2/w for each pellet, that is

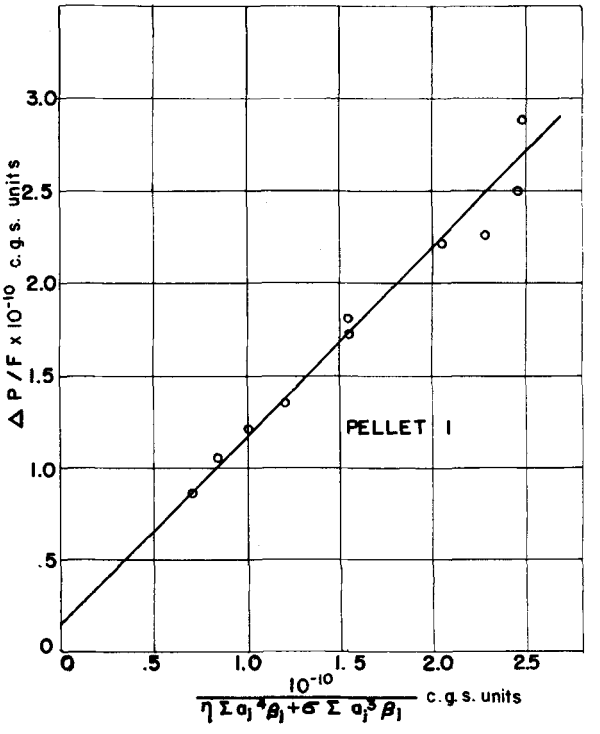

Fig. 6. Flow measurements for calculation of length of diffusion path.

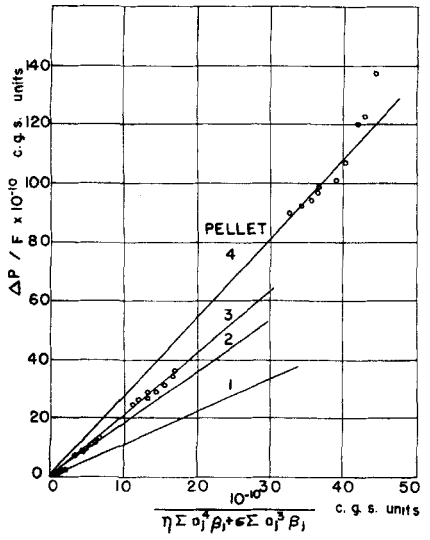

Fig. 7. Flow measurements for calculation of length of diffusion path.

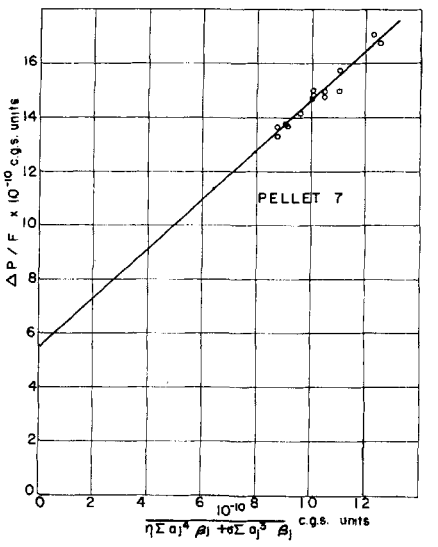

Fig. 8. Flow measurements for calculation of length of diffusion path.

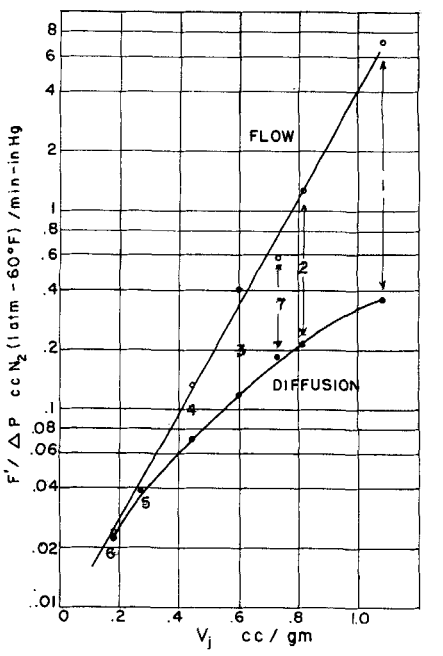

Fig. 9. Comparison of flow and diffusion data.

for pellets of different macropore size distributions.

It should be noted that the flow rate in Equation (15) is based upon unit mass of aluminum oxide in the Boehmite pellet. This is because the pore volume data, and β functions, are on this basis. Thus Figures 1 and 2 give volumes per gram of aluminum oxide. Similarly Equation (10) gives the diffusion rate per gram of aluminum oxide. Hence the path lengths L_B and L_K are on this basis. In contrast actual flow and diffusion data refer to a single pellet. Hence for comparing calculated and experimental results the experimental data were corrected with the pellet masses given in Table 1.

RESULTS

Calculation of Path Lengths

The flow and pore-size distribution data were used to evaluate the path lengths in accordance with Equation (15). A least mean squares technique was used to determine the best straight line through the data. Figure 6 shows the data for pellet 1 and Figure 7 the data for pellets 1, 2, 3, and 4. For all these pellets the intercept is not significantly different from zero. No flow data were obtained on pellet 5. The flow rates for pellet 6 were extremely low, and the results scattered considerably. For this pellet flow data were obtained for both helium and nitrogen and these results used to obtain approximate values of L_K and L_B. Here again the intercepts were approximately zero. Hence it is concluded that for these pellets $L_E = 0$ and diffusion is determined by the macropores. For pellet 7 Figure 8 indicates a finite intercept. This pellet was prepared from a different alumina powder which may have been more susceptible to the formation of relatively nonporous surface layers during pelleting. Values of L_B^2 determined from Equation (15), and the slopes of the lines in Figure 6 to 8, are given in Table 2. What might be termed *actual tortuosities* L_B/(pellet thickness) are also shown in the table. These values range from 1.10 for the least-dense pellet (No. 1) up to 1.71 for the most dense sample (pellet No. 6). The scatter in the flow data for the dense pellets is probably responsible for the fluctuation in actual tortuosities for the more dense samples.

Analysis of Diffusion Data

Diffusion data were obtained on three different pellets of the same density with two or three repeat runs for each pellet. This gave six to nine separate runs on pellets of the same density. Except for the most dense pellet the within-pellet deviation averaged less than 1%. The between-pellet error was about 2 to 3%. The diffusion rates for the most-dense pellet were much lower and varied 5 to 15% from run to run. The average rates per pellet are given for both nitrogen and helium in Table 2.

For comparison purposes Figure 9 shows both diffusion and flow data for nitrogen, plotted as flow rate divided by pressure drop vs. macropore volume. Since the diffusion data were taken at 1 atm. total pressure and the compositions were almost pure helium on one pellet face and pure nitrogen on the other, the partial pressure drop of nitrogen was about 1 atm. Hence comparable flow data would be obtained when the total pressure (only nitrogen present) on one face is atmospheric and on the other face about zero. The mean pressure under these conditions is 0.5 atm. The upper curve in Figure 9 represents the flow data at a mean pressure of 0.5 atm., while the lower curve shows the diffusion data.

If the transport through the catalyst pellet were entirely due to a Knudsen mechanism, comparison of Equations (11) and (3) for Knudsen flow and diffusion would indicate that the curves on Figure 9 should be the same. For the most-dense pellet this appears to be true within experimental error. Figure 2 shows that the maximum-size pore was about 1,000 Å. and the majority of the pores in this pellet were less than 600 Å. The mean free path of nitrogen at the diffusion conditions is about 650Å. (*6*). Thus the physical property data on the pellet suggest that Knudsen diffusion should be expected for this pellet, and this was found to be the case experimentally. However for all other pellets the diffusion and flow rates are different, indicating that diffusion is intermediate between the Knudsen and bulk mechanisms.

Since the macropore volume is the only variable changing from pellet 1 to 6, the data for these pellets should lie on a single curve on Figure 9. However pellet 7 had a considerably different micropore size distribution but still falls close to the curves. This adds further evidence that the macropores are primarily responsible for controlling flow and diffusion through this type of pellet. Similar results were found for diffusion in pelleted silver powders (9). When such materials are used for catalytic reactions, this is not true. Most of the surface is in the micropores, so that diffusion into the micropores is necessary in order to utilize this surface for reaction.

TABLE 2. DIFFUSION DATA AND CALCULATED RESULTS

Pellet no.	Pellet basis: Diffusion rates (g. moles/sec.) × 10^6		L_B^2	Basis 1.0 g. Al_2O_3: L_B/L_p	$L_K/(w)^{1/2}$	Nitrogen diffusion rates × 10^6	
	Nitrogen	Helium	sq. cm.		cm.	Exp. g. moles/sec.	Calc. g. moles/sec.
1	7.25	18.4	1.04	1.10	0	4.77	10.0
2	4.59	11.4	1.66	1.35	0	2.51	4.20
3	2.58	6.56	2.01	1.49	0	1.22	1.96
4	1.50	3.72	2.72	1.81	0	0.616	1.00
5	0.83	2.05	2.77*	1.70	0	0.300	0.588
6	0.46	1.10	2.85	1.71	0	0.144	0.179
7	4.02	10.5	0.95	1.08	0.17	2.45	6.13

Temperature, 80°F.; pressure, 1 atm.

* Interpolated.

Calculated and Experimental Diffusion Rates

Calculated diffusion rates per gram of aluminum oxide for pellets 1 to 7 were obtained from Equation (10). The macropore length L_B was taken from Table 2. These calculated results are shown along with the experimental rates, adapted to the same basis, in the last two columns of Table 2.

The experimental values range from 40 to 80% of the calculated rates. It is advisable at this point to note some of the assumptions inherent in Equation (10) which may account for the difference. First the model supposes that the macro- and micropores can each be represented by a series of cylindrical tubes, all the same length, with no interconnections. The cylindrical shape is a necessary assumption in order to utilize the expressions for diffusion rates developed from kinetic theory and to use the usual results from pore-size distribution measurements. Furthermore Equation (10) is based upon the concept that there are no micropores in parallel with macropores, as far as flow and diffusion paths are concerned. For high-density pellets this assumption is likely to be vulnerable.

In summary the results of this study have shown that:

1. Diffusion through the alumina pellets is a strong function of pellet density, decreasing rapidly as the density, or macropore volume, is lowered.
2. For low density alumina pellets diffusion is controlled by the macropore sizes (for Knudsen contribution) and macropore volume.

ACKNOWLEDGMENT

The authors wish to acknowledge the contribution of Mr. M. F. L. Johnson of Sinclair Research Laboratories, Harvey, Illinois, in measuring the properties of the alumina pellets. The Esso Educational Foundation and the Technological Institute, Northwestern University, provided the financial assistance for this work. The American Cyanamid Company, Stamford, Connecticut, kindly provided the alumina powder and some of its physical properties.

NOTATION

a = radius of pore, cm.
c = concentration, g. moles/cc.
$D_{1,2}$ = bulk diffusivity in a binary system of component 1 and 2, sq. cm./sec.
$D_{K,1}$ = Knudsen diffusivity of component 1, sq. cm./sec.
F = flow rate of nitrogen through pellet, on basis of 1 g. of aluminum oxide g. mole/(sec.) (g. aluminum oxide)
F' = flow rate of nitrogen, cc./min. at 60°F. — 1 atm.
L = pore length; L_K constant length of micropores in model; L_B constant length of macropores in the model, cm.
L_p = pellet thickness, cm.
M = molecular weight
N = diffusion flux, g. moles/(sec.) (sq. cm.)
n = number of pores of a particular radius per gram of aluminum oxide
P = total pressure, g./(cm.) (sec.^{2})
p = partial pressure, g./(cm.) (sec.^{2})
Q_1 = diffusion rate of nitrogen through pellet, on basis of 1.0 g. of aluminum oxide, g. moles/(sec.) (g. aluminum oxide)
T = temperature, °K.
V = volume in pores, per gram of aluminum oxide, cc/(g. aluminum oxide)
$\bar{v}$ = average molecular speed, cm./sec.
w = fraction of micropores in the stressed ends of the pellet
x = mole fraction
z = diffusion or flow distance, cm.

Greek Letters

α = ratio of fluxes of components 2 (helium) and 1 (nitrogen)
β = n_iL_K for micropores and n_jL_B for macropores, cm.
γ = defined by Equation (4), sec. (g. mole)/(g.) (cm.)
ϵ = void fraction
η = defined by Equation (13), g. mole (sec.)/(sq. cm.) (g.)
σ = defined by Equation (14), sec. (g. mole)/(g.) (cm.)
μ = viscosity, g./(cm.) (sec.)

Subscripts

1,2 = components nitrogen and helium, respectively
i = micropore of radius a_i
j = macropore of radius a_j
K = Knudsen flow or micropore region
B = macropore region
o = outer end of micropore region (Figure 5)
I = boundary between micro- and macropore regions (Figure 5)
L = outer end of macropore region (Figure 5)

LITERATURE CITED

1. Beek, John, *A.I.Ch.E. Journal*, 7, 337 (1961).
2. Carberry, J. J., *ibid.*, p. 350
3. Evans, R. B., G. M. Watson, and E. A. Mason, *IMP-AEC-15*, Institute for Molecular Physics, University of Maryland, College Park, Maryland (1961).
4. de Boer, J. H., Colston Papers, No. 10, "Structure and Properties of Porous Materials," Academic Press, New York (1959).
5. Henry, J. P., Balapa Chennakesavan, and J. M. Smith, *A.I.Ch.E. Journal*, 7, 10 (1961).
6. Hirschfelder, J. O., C. F. Curtiss, and R. B. Bird, "Molecular Theory of Gases and Liquids," Chap. 1, p. 15, Wiley, New York (1954).
7. Hoogschagen, J., *Ind. Eng. Chem.*, 47, 906 (1955).
8. Present, R. D., "Kinetic Theory of Gases," McGraw-Hill, New York (1958).
9. Masamune, S., and J. M. Smith, *A.I.Ch.E. Journal*, 8, 217 (1962).
10. Mingle, J. O., and J. M. Smith. *A.I.Ch.E. Journal*, 7, 243 (1961).
11. Rothfeld, L. B., Ph.D. thesis, University of Wisconsin, Madison, Wisconsin (1961).
12. Scott, D. S., and F. A. Dullien, *A.I.Ch.E. Journal*, 8, 113 (1962).
13. Weisz, P. B., Z. *Physik. Chem.*, 11, 1 (1957).
14. Wheeler, A., "Catalysis," Vol. 2, p. 105, Reinhold, New York (1955).
15. Wicke, E., and R. Kallenbach, *Kolloid-Z.*, 97, 135 (1941).

Manuscript received July 13, 1961; revision received August 22, 1962; paper accepted August 24, 1962. Paper presented at A.I.Ch.E. New York meeting.